A two-phase two-dimensional finite element thermomechanics and macrosegregation model of mushy zone. Application to continuous casting

Michel Bellet, Victor D. Fachinotti

Proc. MCWASP XI, 11th Int. Conf. on Modeling of Casting, Welding and Advanced Solidification Processes, Opio, France, May 28 - June 3, 2006, C.A. Gandin, M. Bellet (eds.), The Minerals, Metals & Materials Society, Warrendale, Pennsylvania, USA (2006) 169-176

A TWO-PHASE TWO-DIMENSIONAL FINITE ELEMENT THERMOMECHANICS AND MACROSEGREGATION MODEL OF MUSHY ZONE. APPLICATION TO CONTINUOUS CASTING

Michel Bellet[1], Victor D. Fachinotti[2]

[1] Ecole des Mines de Paris, CEMEF, UMR CNRS 7635, Sophia Antipolis, France
[2] Centro Internacional de Métodos Computacionales en Ingenieria (CIMEC-CONICET), Parque Tecnologico del Litoral Centro, S3007 ABA Santa Fe, Argentina

Keywords: solidification, mushy zone, 2-phase, thermomechanics, finite elements

Abstract

The main lines of a coupled thermomechanical - solute transport model are first summarized. Macroscopic conservation equations for mass, momentum, energy and solute are obtained by a spatial averaging method. The mechanical model is a "sponge-like" one: assuming a semi-solid saturated mushy zone, the solid phase is macroscopically modeled as a compressible viscoplastic continuum, while the liquid phase flow obeys Darcy's law. Regarding solute transport, the study is limited to a binary alloy for which the solidification path is not given a priori but results from a microsegregation model (here the lever rule). A validation check of the correct implementation of this coupled model is achieved by comparing with an analytical solution in the case of a free compression of a saturated semi-solid medium. Application to the study of the solidification during secondary cooling in steel continuous casting is considered.

Introduction

Macrosegregation is a central issue in solidification engineering, because it determines the further processibility and final properties of cast products. In most cases, it results from slow interdendritic flow, driven by thermo-solutal convection. Generally, the influence of the solid motion on fluid flow is assumed of minor importance and, as a matter of fact, most casting numerical simulations neglect this phenomenon. However, as demonstrated by Flemings [1], in some cases, macrosegregation highly depends on the deformation of the solid skeleton forming in the mushy zone. This is especially the case in continuous casting (but not exclusively) where there exists a large mushy zone, which is deformed together with the solid shell because of the bulging between the supporting rolls of the caster. This problem has already been addressed by several authors. Following the pioneer work of Miyazawa and Schwerdtfeger [2], and the analytical developments of Lesoult and Sella [3], Kajitani et al. [4] proposed a more advanced numerical model. However in their approach they did not take into account the deformation of the solid phase in the mushy zone and made strong hypotheses on its velocity field. The present work is a contribution to address such complex phenomena. It is focused on the deformation of a coherent mushy zone, i.e. in which the solid fraction is higher than the coherency fraction, which is the fraction over which the solid phase is continuous and able to transmit stresses higher than those in the liquid. The mushy zone is considered here as an effective two-phase continuum. On one hand, the solid material is considered as an incompressible viscoplastic material, obeying a constitutive equation of power-law type. Invoking homogenization results, its macroscopic flow rule is viscoplastic, including compressibility, so that the solid continuum can be seen as a deformable compressible porous medium. On the other hand, the liquid phase

is intrinsically Newtonian. At the macroscopic scale, its momentum interaction with the solid skeleton is of Darcy type. Thus, the present thermomechanical approach is similar to the one of M'Hamdi et al [5] to study hot tearing issues in aluminium continuous casting. However, the present model involves a full coupling with macrosegregation equations. A two-dimensional finite element implementation of the corresponding mass, momentum, energy and solute conservation equations has been carried out: see references [6, 7] for a complete description.

Macroscopic Two-Phase Model

Governing Equations

At the microscopic scale, inside each phase, the thermo-mechanical evolution is assumed to be governed by the usual mass, momentum energy and solute balances. In this work, the balance equations of the mixture, at the macroscopic scale of a representative elementary volume (REV), are obtained using the spatial averaging method (not detailed here, see [8, 9] for further details and usual notations). The solidifying alloy in the mushy state is considered as a saturated two-phase medium ($g_s + g_l = 1$). Applying the averaging process to microscopic balance equations in each phase k ($k = s, l$), the following set of macroscopic equations is obtained.

$$
\begin{aligned}
&\textit{Mass} && \frac{\partial}{\partial t}(g_k \rho_k) + \nabla \cdot (g_k \rho_k \boldsymbol{v}_k) = \Gamma_k \\
&\textit{Momentum} && \nabla \cdot (g_k \boldsymbol{\sigma}_k) + \boldsymbol{M}_k + g_k \rho_k \boldsymbol{g} = \frac{\partial}{\partial t}(g_k \rho_k \boldsymbol{v}_k) + \nabla \cdot \left(g_k \rho_k \boldsymbol{v}_k \times \boldsymbol{v}_k\right) \\
&\textit{Energy} && \frac{\partial}{\partial t}\left(g_k \rho_k h_k\right) + \nabla \cdot \left(g_k \rho_k h_k \boldsymbol{v}_k\right) + \nabla \cdot \left\langle \boldsymbol{q}^k \right\rangle = Q_k \\
&\textit{Solute} && \frac{\partial}{\partial t}\left(g_k c_k\right) + \nabla \cdot \left(g_k c_k \boldsymbol{v}_k\right) + \nabla \cdot \left\langle \boldsymbol{j}^k \right\rangle = J_k
\end{aligned}
\qquad (1)
$$

where ρ denotes the density, $\boldsymbol{v}$ the velocity field, $\boldsymbol{\sigma}$ the stress tensor, $\boldsymbol{g}$ the gravity vector, h the enthalpy per unit of mass, $\boldsymbol{q}$ the heat flow vector, c the volume concentration, $\boldsymbol{j}$ the solute flow vector. The terms Γ, $\boldsymbol{M}$, Q and J are associated with the exchanges of mass, momentum, energy and solute, respectively, between the two phases.

Mass and momentum conservation. The local mass balance at the interface between phases ensures that $\Gamma_s + \Gamma_l = 0$. Summing equations (1a) for the liquid and solid phase, and assuming that the phase densities remain constant but different in the solidification interval, we get:

$$
\frac{\rho_s}{\rho_l} \nabla \cdot (g_s \boldsymbol{v}_s) + \nabla \cdot (g_l \boldsymbol{v}_l) = \frac{\rho_l - \rho_s}{\rho_l} \frac{\partial g_s}{\partial t} \qquad (2)
$$

The spatial averaging method is efficient to obtain in a simple way the macroscopic governing equations but does not enable to go further in the specifications of the macroscopic model. Reliable constitutive equations would require more sophisticated approaches such as homogenization [10] associated with numerical simulation at the microscopic scale, but this is not in the scope of this work. The full definition of the two-phase model will simply be based on the following constitutive assumptions.

At the microscopic scale, the liquid metal is assumed to behave as an incompressible Newtonian fluid. This is expressed by

$$\boldsymbol{\sigma} = \boldsymbol{s} - p\boldsymbol{I} = 2\mu_l\, \dot{\boldsymbol{\varepsilon}}(\boldsymbol{v}) - p\boldsymbol{I} \tag{3}$$

where p denotes the hydrostatic pressure, $\boldsymbol{s}$ the deviatoric part of $\boldsymbol{\sigma}$, μ_l the viscosity of the liquid, and $\dot{\boldsymbol{\varepsilon}}(\boldsymbol{v})$ the strain rate tensor. Like Ganesan and Poirier [11] and Rappaz et al. [9], we adopt the following model for the macroscopic deviatoric stress tensor in the liquid phase:

$$\boldsymbol{\Sigma}^l = \left\langle \boldsymbol{s}^l \right\rangle = 2\mu_l\, g_l\, \mathrm{dev}\left(\dot{\boldsymbol{\varepsilon}}(\boldsymbol{v}_l)\right) = 2\mu_l\, g_l \left(\dot{\boldsymbol{\varepsilon}}(\boldsymbol{v}_l) - \frac{1}{3}\mathrm{tr}(\dot{\boldsymbol{\varepsilon}}(\boldsymbol{v}_l)) \right) \tag{4}$$

Regarding the solid phase, its microscopic behavior at very high temperature can be modeled by the Norton-Hoff constitutive equation:

$$\boldsymbol{\sigma} = \boldsymbol{s} - p\boldsymbol{I} \quad \text{with} \quad \boldsymbol{s} = 2K(\sqrt{3}\dot{\varepsilon}_{eq})^{m-1}\, \dot{\boldsymbol{\varepsilon}}(\boldsymbol{v}) \tag{5}$$

where K and m denote the consistency and the strain rate sensitivity and $\dot{\varepsilon}_{eq}$ the von Mises equivalent strain rate. Using results from homogenization theory [10], the effective stress tensor $\boldsymbol{\Sigma}^s = \left\langle \boldsymbol{s}_s \right\rangle - \left\langle p_s \right\rangle \boldsymbol{I} + g_s\, p_l \boldsymbol{I}$ is shown to be a degree m homogeneous function with respect to the strain rate tensor $\left\langle \dot{\boldsymbol{\varepsilon}} \right\rangle^s = \dot{\boldsymbol{\varepsilon}}(\boldsymbol{v}_s)$. This property shows that the solid phase can be modeled as a compressible power law fluid. We therefore adopt a compressible viscoplastic formalism [12], yielding the following constitutive equation:

$$\boldsymbol{\Sigma}^s = 3K(\sqrt{3}\left\langle \dot{\varepsilon} \right\rangle_{eq}^s)^{m-1} \left(\frac{1}{A}\left\langle \dot{\boldsymbol{\varepsilon}} \right\rangle^s + \left(\frac{1}{9B} - \frac{1}{3A} \right) \mathrm{tr}\left\langle \dot{\boldsymbol{\varepsilon}} \right\rangle^s \boldsymbol{I} \right) \tag{6}$$

in which the two rheological functions A and B depend on the solid volume fraction, according to different models [12]. Unlike (5), the equivalent strain rate is now expressed as:

$$\left\langle \dot{\boldsymbol{\varepsilon}} \right\rangle_{eq}^{s\ 2} = \frac{1}{A}\left\langle \dot{\boldsymbol{\varepsilon}} \right\rangle^s : \left\langle \dot{\boldsymbol{\varepsilon}} \right\rangle^s + \left(\frac{1}{9B} - \frac{1}{3A} \right) \left(\mathrm{tr}\left\langle \dot{\boldsymbol{\varepsilon}} \right\rangle^s \right)^2 \tag{7}$$

This model permits a first introduction of the compressibility of the solid skeleton. It is worth noting that in a recent work, Ludwig et al. [13] suggest to complement such a simple model with a state variable representing the cohesion of the skeleton, allowing a better response for small deformations, such as those encountered in continuous casting.

Finally, regarding the exchange of momentum, $\boldsymbol{M}_k$ is the sum of the contributions of deviatoric stresses and pressure [8]. Assuming that the interfacial pressures in both phases equal the intrinsic average value of liquid pressure, and that the liquid interstitial flow is governed by the Darcy law (isotropic permeability K), we have:

$$\boldsymbol{M}_l = -\boldsymbol{M}_s = \frac{g_l^{\ 2}\mu_l}{\mathrm{K}} \left(\boldsymbol{v}_l - \boldsymbol{v}_s \right) + p_l \nabla g_l \tag{8}$$

Energy conservation. Assuming the local thermal equilibrium assumption ($T_s = T_l = T$), the classic equation for the energy conservation in the mixture is considered:

$$\frac{\partial}{\partial t}\left\langle \rho h \right\rangle + \nabla \cdot \left\langle \rho h \boldsymbol{v} \right\rangle + \nabla \cdot \left\langle \boldsymbol{q} \right\rangle = 0 \tag{9}$$

Defining the enthalpies of solid and liquid as follows, $h_s = \int_{T_0}^{T} c_p(\tau) d\tau$ and $h_l = h_s + L$, it can be shown [7] that (9) can be cast in the form:

$$\langle\rho\rangle \frac{\partial\langle h\rangle}{\partial t} + c_p \nabla T \cdot \langle\rho \boldsymbol{v}\rangle + L\left(\rho_l \nabla \cdot \left\langle \boldsymbol{v}^l \right\rangle - f_l \nabla \cdot \langle\rho \boldsymbol{v}\rangle\right) - \nabla \cdot (\langle\lambda\rangle \nabla T) = 0 \tag{10}$$

Solute conservation. In a first approach, the local lever rule is adopted to model microsegregation. It provides a direct relation between the liquid and solid volume concentrations ($c_s = k c_l$). The resolution consists then in solving the equation of solute conservation in the mixture (assuming Fick's law in the liquid and neglecting the macroscopic diffusion effects in the solid) [7]:

$$\frac{\partial\langle c\rangle}{\partial t} + \nabla \cdot (\langle c\rangle \boldsymbol{v}_s) + \nabla \cdot (g_l c_l (\boldsymbol{v}_l - \boldsymbol{v}_s)) - \nabla \cdot (g_l D_l \nabla c_l) = 0 \tag{11}$$

After resolution for the average concentration, the liquid fraction, temperature, and liquid and solid concentration can be recovered by solving a non linear equation in each node.

Numerical Implementation

The final equation set is composed of five equations: (1b) for solid, (1b) for liquid, (2), (10) and (11). The weak forms of those equations are spatially discretized using P1 triangle elements [6, 7]. At each time increment, the successive conservation problems are solved: energy, solute, momentum (liquid and solid), mass. Momentum and mass conservations are solved together using a velocity-pressure formulation in which the nodal unknowns are $\boldsymbol{v}_l$, $\boldsymbol{v}_s$, p_l.

Validation of the 2-Phase Liquid-Solid Mechanical Resolution

The homogeneous plane strain simple compression problem depicted in Figure 1 is considered. The solid phase behavior is assumed linear ($m = 1$ in Eq. (6)). The liquid fraction is assumed uniform. This produces a simple-compression-like kinematics for both phases with an imposed strain rate $\dot{\varepsilon} = |V_{imp}| / h$. The normal stress on each phase is supposed to be null on the lateral vertical faces. Contact is assumed perfectly sliding. An analytical resolution [7] leads to the following expressions for the phase velocities and liquid pressure:

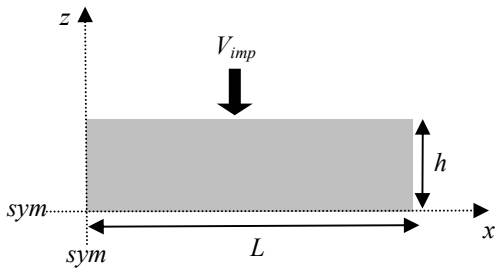

Figure 1. Two-phase simple compression test geometry.

$$\begin{cases} v_{s_x}(x) = \dot{\varepsilon} x + a_0 \sinh(rx) \qquad v_{l_x}(x) = \dot{\varepsilon} x - \dfrac{g_s}{g_l} a_0 \sinh(rx) \qquad v_{s_z}(x) = v_{l_z}(x) = 0 \\ p_l(x) = \left(\dfrac{3}{A} K_s + 2\mu_l g_l\right)\dot{\varepsilon} + \left(K_s\left(\dfrac{1}{3B} + \dfrac{2}{A}\right) - \dfrac{4}{3} g_s \mu_l\right) a_0 r \cosh(rx) \end{cases} \tag{12}$$

with $$r = \sqrt{\frac{g_l \mu_l}{\mathrm{K}\tilde{\mu}}} \qquad a_0 = \frac{g_l\left(2 g_s \mu_l - \dfrac{3}{A} K_s\right)}{\tilde{\mu} r \cosh(rL)} \dot{\varepsilon} \qquad \tilde{\mu} = g_l K_s\left(\frac{1}{3B} + \frac{2}{A}\right) + \frac{4}{3} {g_s}^2 \mu_l \tag{13}$$

Results exposed Figure 2 and Figure 3 correspond to conditions that are representative of the mechanical solicitation applied to the mushy core of a steel slab during secondary cooling when passing between support rolls. Dimensions and parameters are given in Table I. Figure 2 shows the influence of the permeability, by considering a variation of the secondary dendrite arm spacing λ_2. For instance, a decrease of λ_2 induces a decrease of the permeability: the relative velocity is diminished while the liquid pressure increases. The results of the 2-phase finite element model match exactly the closed form solution, as illustrated in Figure 3.

Table I. Dimensions and parameters used in the validation test.

$L = 0.25$ m	$V_{imp} = 10^{-3}$ m/s	$\mu_l = 10^{-3}$ Pa s	$A = 20$	$\lambda_2 = 150\times10^{-6}$ m	$K = \dfrac{\lambda_2^{\,2} g_l^{\,3}}{180(1-g_l)^2}$
$h = 0.1$ m	$g_s = 0.8$	$K_s = 10^{7}$ Pa s	$B = 0.5$		

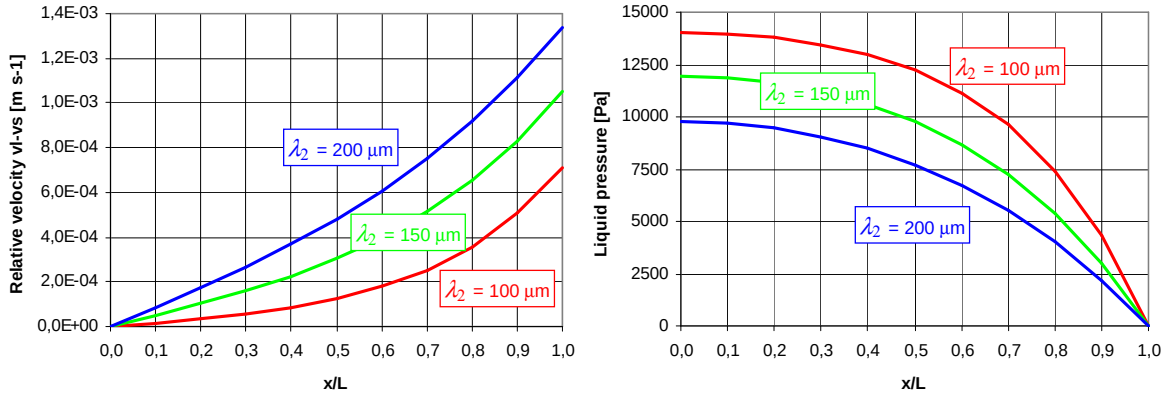

Figure 2. Results of the analytical model, showing the influence of permeability.

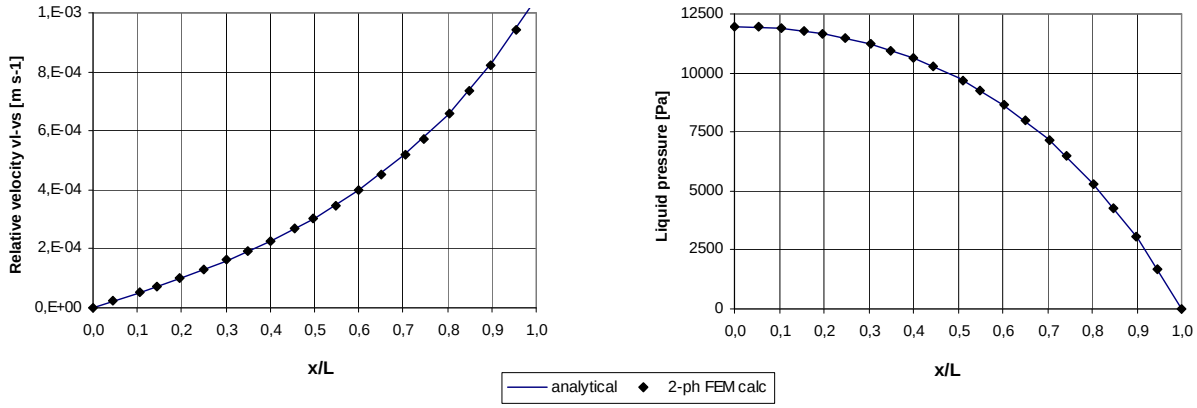

Figure 3. Comparison between 2-phase FEM solution and reference analytical solution.

Application to Steel Continuous Casting

The material is modeled as a binary Fe-0.18wt%C alloy. The casting velocity is 0.86 m/min and the product thickness is 222 mm. In order to apply the two-phase formulation to a coherent mushy zone, we proceed in two steps. In a first step, a classical "one-phase-like" thermo-mechanical analysis is performed [14]. The result of such a calculation is shown in Figure 4. Then we can determine at which depth in the machine the mushy core is fully coherent, i.e. when the solid fraction is greater than 0.65. In a second step, we initialize the two-phase calculation starting from this section (Figure 5). As in step 1, the computational mesh will grow at the casting speed, starting from a small mesh that serves as a buffer in the simulation. Along the inlet section of this buffer, the profile of average enthalpy is imposed (resulting from step 1) together with the normal stress expressing the metallostatic load. In addition, a uniform nominal solute concentration is assumed, expressing the hypothesis that no segregation has formed yet.

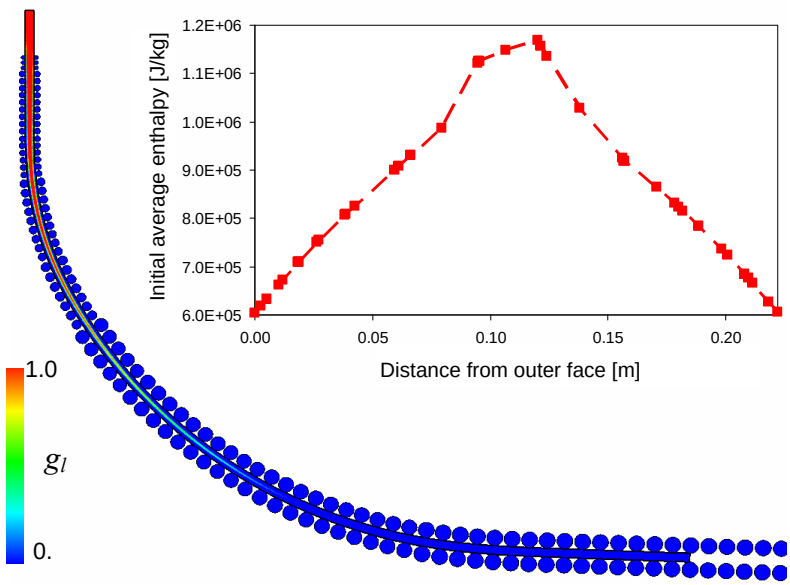

Figure 4. Step 1: thermomechanical stress-strain analysis, using a "one-phase-like" approach in order to provide relevant information to initiate step2 (two-phase calculation). Distribution of liquid fraction. The chart is the enthalpy profile in the section at 11 m below the meniscus, which is used as an initial condition for the two-phase calculation.

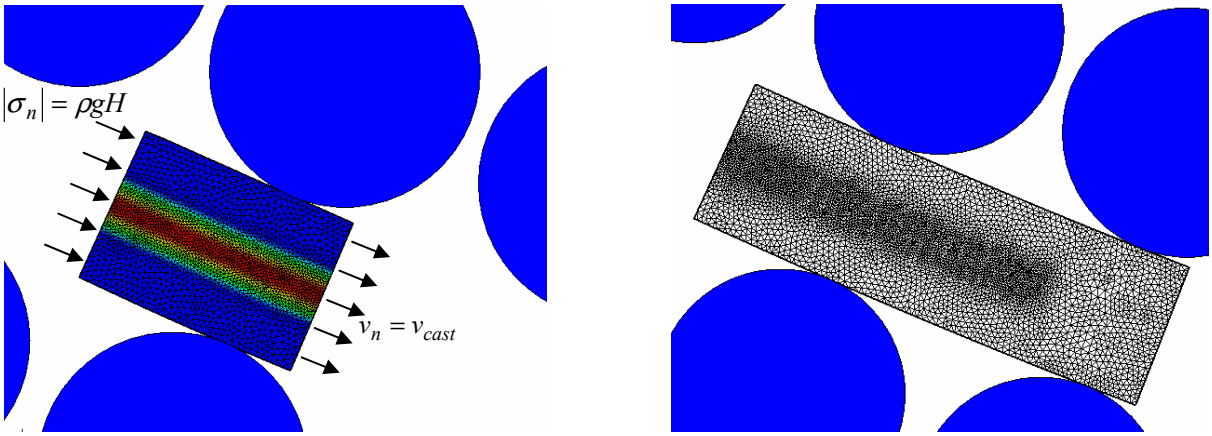

Figure 5. Step 2: boundary conditions and growth of the mesh (refined in the center of product).

A first calculation was done with a magnified bulging between rolls. This is obtained by dividing the viscoplastic consistency of the fully solid material by a factor 10. The solid phase being assumed coherent all along the analysis, its deformation remains small. Thus, the velocity field assigned to the finite element mesh is the intrinsic solid velocity. The mesh is then attached to the solid skeleton and does not need any remeshing. Figure 6 shows the typical fluid flow in the mushy zone as calculated by the 2-phase formulation. It is worth noting the impact of bulging and compression between rolls. In the bulging zone, the center of the mushy zone is submitted to tensile stresses. This produces an expansion of the solid skeleton ($\nabla \cdot \boldsymbol{v}_s > 0$) associated with a liquid flow towards the center of the mushy zone. Conversely, between two rolls, the central region of the mushy zone is compressed ($\nabla \cdot \boldsymbol{v}_s < 0$), expelling the liquid phase towards the solidification front.

In the real process, when the bulging is reduced to about 1 mm, the liquid redistribution is less pronounced although it is thought to be responsible for macrosegregations. The modeling has been carried out using the nominal viscoplastic consistency. The computational domain extends up to a section located at a casting distance of 3.25 m, as shown in Figure 7.

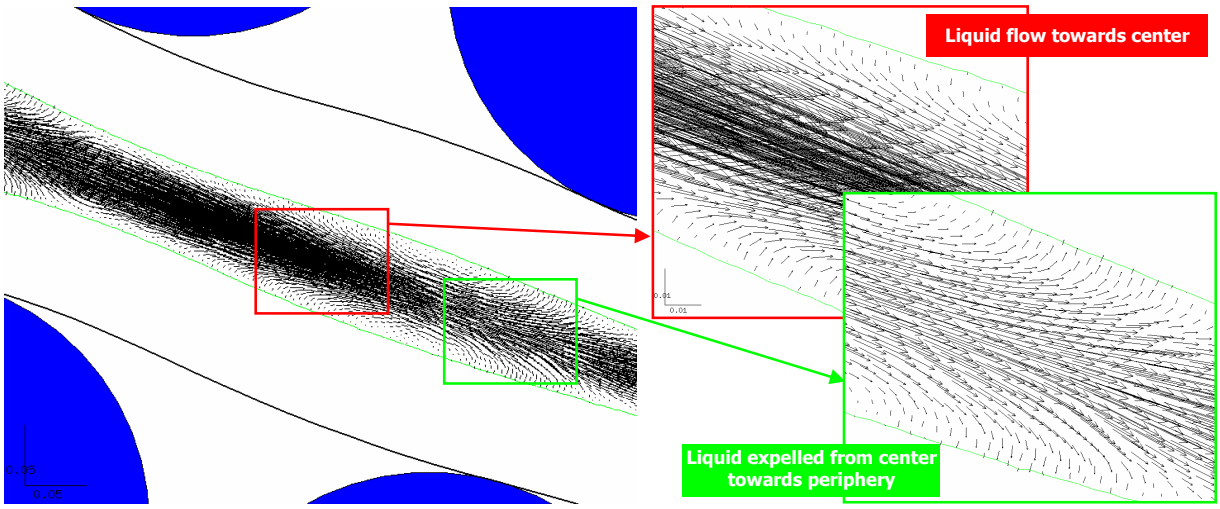

Figure 6. Case with artificial magnification of bulging. Relative velocity vectors $\boldsymbol{v}_l - \boldsymbol{v}_s$ in the mushy core of the slab, limited by the solidus isotherm.

Regarding macrosegregation, the final carbon segregation $\langle c \rangle - c_0$ is depicted in Figure 7, showing the ability of the model to capture the phenomenon of central (positive) segregation. It is worth noting a deviation of the concentration peak from the middle of the slab, which might result from gravity and slab curvature. Even if the solidification is not complete, so that the solute concentrations can still evolve, the computed level of macrosegregation seems to be significantly lower than in reality. Nevertheless, it can be thought that this result should be significantly improved by using more realistic constitutive models and parameters, especially for the solid phase compressible behavior and the mechanical interaction term. These points are being investigated, as well as the sensitivity to the finite element mesh size.

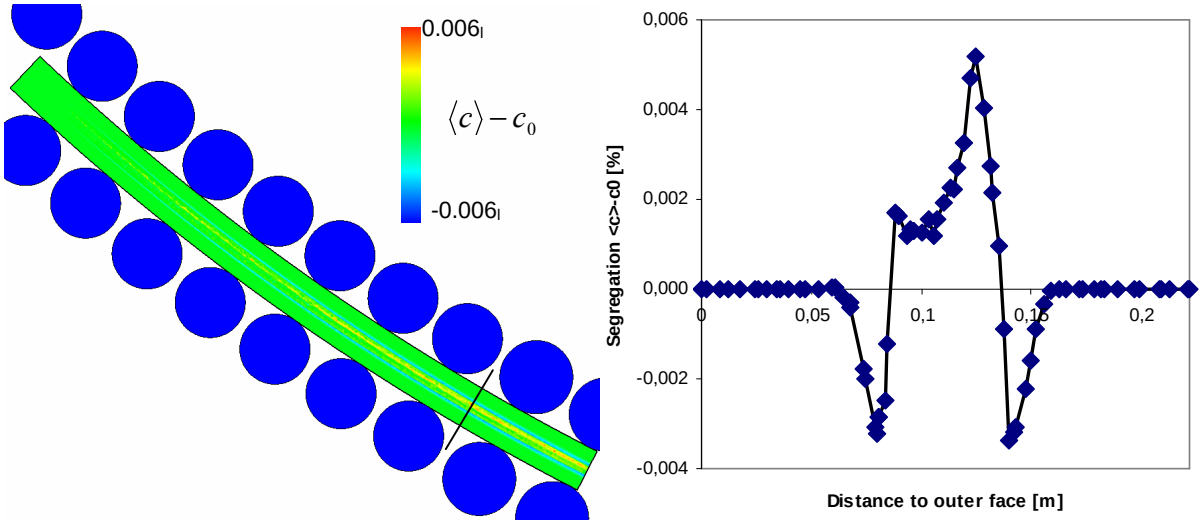

Figure 7. On the left, computed domain at the end of Step2 calculation, with the map of carbon segregation (deviation from nominal concentration). On the right, carbon concentration in a transverse section of the slab (as indicated in the left part of the figure).

Conclusion

In this paper, the macroscopic conservation equations for a two-phase continuum have been briefly discussed and summarized. A two-dimensional finite element resolution has been proposed and validated on an analytical test. The ability of the formulation to represent the deformation of a saturated solid skeleton, using a “sponge-like” model has been demonstrated.

Its application to the simulation of the secondary cooling of continuous casting should provide a powerful tool for the understanding and control of defects such as central macrosegregations.

References

1. M.C. Flemings, "Our understanding of macrosegregation: past and present", ISIJ Int. 40 (2000) 833-841.

2. K. Miyazawa, K. Schwerdtfeger, "Macrosegregation in continuously cast steel slabs: preliminary theoretical investigation on the effect of steady state bulging", Arch. Eisenhüttenwes. 52 (1981) 415-422.

3. G. Lesoult, S. Sella, "Analysis and prevention of centreline segregation during continuous casting of steel related to deformation of the solid phase", Proc. 6th Int. Iron and Steel Congress, Nagoya, Iron and Steel Institute of Japan, vol. 1 (1990) 681–688.

4. T. Kajitani, J.M. Drezet, M. Rappaz, "Numerical simulation of deformation induced segregation in continuous casting of steel", Metall. and Mater. Trans. A 32 (2001) 1479-1491.

5. M. M'Hamdi, A. Mo, C. L. Martin, "Two-phase modeling directed toward hot tearing formation in aluminum direct chill casting", Metall. Mater. Trans. A 33 (2002) 2081-2093.

6. M. Bellet, S. Le Corre, V.D. Fachinotti, "A 2-phase finite element model to study concurrent fluid flow and solid deformation occurring in mushy zones during the solidification of metallic alloys", Proc. S2P, Int. Conf. on Semi-Solid Processing of Alloys and Composites, CDROM, University of Cyprus and Worcester Polytechnic Institute (USA), 9 pages (2004).

7. M. Bellet, V.D. Fachinotti, S. Le Corre, N. Triolet, M. Bobadilla, "Two-phase thermo-mechanical and macrosegregation modelling of binary alloys solidification with emphasis on the secondary cooling stage of steel slab continuous casting", submitted to Int. J. Num. Meth. Eng. (2005).

8. J. Ni, C. Beckermann, "A volume-averaged two-phase model for transport phenomena during solidification", Metall. Trans. B 22 (1991) 349-361.

9. M. Rappaz, M. Bellet, M. Deville, Numerical modelling in materials science and engineering, Springer Verlag, New York, (2003).

10. C. Geindreau, J.L. Auriault, "Investigation of the viscoplastic behaviour of alloys in the semi-solid state by homogenization", Mechanics of Materials 31 (1999)535-551.

11. S. Ganesan, D.R. Poirier, "Conservation of mass and momentum for the flow of interdendritic liquid during solidification", Metall. Trans. B 21 (1990) 173-181.

12. T.G. Nguyen, D. Favier, M. Suéry, "Theoretical and experimental study of the isothermal mechanical behaviour of alloys in the semi-solid state", Int. J. Plasticity 10 (1994) 663-693.

13. O. Ludwig, B. Commet, J.M. Drezet, C.L. Martin, M. Suéry, "Rheological behavior of partially solidified Al-Cu alloys : experimental and numerical study", Proc. MCWASP X, 10th Int. Conf. on Modeling of Casting, Welding and Advanced Solidification Processes, The Minerals, Metals & Materials Society, Warrendale, Pennsylvania, USA (2003) 183-190.

14. M. Bellet, A. Heinrich, "A two-dimensional finite element thermomechanical approach to a global stress-strain analysis of steel continuous casting", ISIJ Int. 44 (2004) 1686-1695.

Acknowledgements

The authors would like to acknowledge the financial support of Arcelor Research SA. Victor D. Fachinotti was also granted by the Argentine Council for Scientific and Technical Research (CONICET) during its stay at CEMEF laboratory.